

Evaluation of Inexpensive Capacitive Soil Moisture Sensors for IoT Networks

Abstract:

An experiment was conducted at G D Goenka University to assess the effectiveness of low-cost capacitive soil moisture sensors in diverse soil samples from various geographic regions. This study explores the potential of integrating such sensors into IoT networks. The rapid proliferation of IoT technology has prompted advancements in greenhouse technology and agriculture, emphasizing automation and data-driven decision-making. The precise measurement of soil moisture is crucial across multiple scientific disciplines, including agronomy, soil physics, geology, hydraulics, and soil mechanics. This paper focuses on characterizing a commercially available, cost-effective capacitive coplanar soil moisture sensor suitable for deployment in distributed IoT nodes. Our findings indicate that this capacitive sensor establishes a dependable correlation between output voltage and gravimetric water content, particularly in soils with a consistent solid-to-volume ratio.

Keywords: moisture sensor, capacitive measurement, low-cost capacitive moisture sensor, soil water content measurement techniques, geotechnical investigation, SKU: SEN0193 sensor.

Introduction:

The development of the Internet of Things (IoT) signifies the creation of a global network comprising intelligent entities, or "things," equipped with sensors, typically microcontrollers enhanced with networking capabilities. Within this framework, communication technologies offer the potential to revolutionize current monitoring methods, enabling real-time responses across a broad spectrum of applications (Perera *et al.*, 2014; Rajab and Cinkelr, 2018; Zgank, 2019; Saab *et al.*, 2019). Sensors are designed to gather diverse data, including temperature, pressure, light, humidity, and soil moisture. On the other hand, microcontrollers with networking capabilities possess the capacity to process, store, and interpret this data, forming intelligent wireless sensor networks (WSNs)(Ruiz-Garcia *et al.*, 2009; Magalottiet *al.*, 2016; Khan *et al.*, 2020).WSNs have found widespread applications in agriculture since their introduction in the early 21st century (Wang *et al.*, 2006; Surendran *et al.*, 2019). A notable advantage of wireless transmission is its ability to significantly reduce and simplify the wiring and cabling required for

various applications, a particularly crucial feature in smart farming (González-Teruel *et al.*, 2019; Beecham, 2020), where the flexibility of sensor placement is essential. Earlier works have already outlined a modular IoT architecture for various applications, encompassing domains such as healthcare, health monitoring, and precision agriculture (Yelamarthi *et al.*, 2017; Zyrianoff *et al.*, 2020). In this context, soil moisture or water content assumes considerable significance. Water is recognized as one of the most vital resources for sustainable development, given its growing demand in irrigated regions, urban areas for domestic use, and industrial applications in the upcoming years. Moreover, irrigation efficiency is often suboptimal, with only a fraction of crops effectively utilizing irrigation water. Consequently, the sustainable use of irrigation water is a primary concern for agriculture, particularly in water scarcity scenarios. Numerous efforts have been dedicated to enhancing water efficiency, guided by the principle that "achieving more with less water is feasible through improved management" (Chartzoulakisa and Bertaki, 2015). The modernization and automation of irrigation systems call for deploying sensor-based equipment. Conventionally, sensor data monitor environmental conditions and soil water status, offering insights into the overall crop water requirements (Torres-Sanchez *et al.*, 2020). Among the most commonly employed soil parameter sensors are those based on dielectric properties, valued for their cost-effectiveness and adaptability (Campbell, 1990; Visconti *et al.*, 2014). However, their accurate operation necessitates intricate calibration that considers factors such as soil texture, structure, temperature, and water salinity (González-Teruel *et al.*, 2019; Visconti *et al.*, 2014; Kizito *et al.*, 2008; Kargas and Soulis, 2019), as well as accounting for the spatial variability of soil conditions (Barker *et al.*, 2017). Additionally, thermal and multispectral cameras, satellites, and infrared radiometers (IR) are employed to estimate crop water requirements (Gavilán *et al.*, 2019; Jackson *et al.*, 1999; García-Tejero *et al.*, 2018; Jackson *et al.*, 1981).

However, precise and experimental determination of soil moisture remains critically important in various scientific disciplines, including agronomy, soil physics, geology, hydraulics, and soil mechanics. The soil water content significantly impacts physical, chemical, mineralogical, and biological properties. A comprehensive overview of soil moisture measurement techniques has been previously documented (Whalley *et al.*, 1992; Su *et al.*, 2014; Tarantino *et al.*, 2008 (a); Tarantino *et al.*, 2008 (b)). The thermo-gravimetric method represents the classical approach for determining soil moisture in geotechnical engineering applications. Modern techniques

encompass soil resistivity measurement, neutron scattering, tensiometers, infrared moisture balance, dielectric methods such as frequency domain reflectometry, time domain reflectometry, heat flux soil moisture sensors, optical techniques, and contemporary micro-electromechanical systems. Notably, several reviews on dielectric methods have been published in the literature (Gardner *et al.*, 2000; Noborio *et al.*, 1994; Robinson *et al.*, 2003).

Our study is centered on the experimental evaluation of a low-cost commercial "capacitive" soil moisture sensor that can be integrated into distributed nodes for IoT applications. Our objective is to verify its performance and reliability in determining soil physical properties. Given the necessity for a large-scale deployment of IoT sensor nodes while minimizing component costs, we have chosen the SKU:SEN0193 sensor, as it is the most affordable and readily available in the market. However, comprehensive information about the sensor's operation is lacking. Therefore, it is valuable to assess its performance and understand its limitations, both for irrigation management and soil moisture determination, particularly in geotechnical applications. To the best of our knowledge, the sensor investigated in this study has only been characterized once before (Nagahage *et al.*, 2019), during a laboratory evaluation of its accuracy and reliability. In that study, the sensor was found to perform inadequately in predicting soil moisture content in a laboratory soil mixture comprising organic-rich soil and vermiculite. However, it demonstrated reasonable performance in estimating soil water content in gardening soil within the "field capacity" range. In this paper, we provide a detailed analysis of the sensor's electrical circuit and a statistical assessment involving several nominally identical samples to gain a better understanding of its limitations and suitability when used with silica sandy soil.

Material and methods:

Evaluation of Inexpensive Capacitive Soil Moisture Sensors for IoT Networks was conducted at the Agronomy Lab at G. D. Goenka University with the following materials and methods.

Soil Water Content Measurements:

The presence of water is undeniably a critical factor influencing the chemical, physical, and mechanical characteristics of soil. Soil moisture content, especially in the upper layers close to the water table, significantly impacts plant growth, the organization of natural ecosystems, and overall biodiversity. In the agricultural domain, the judicious application of timely irrigation,

tailored to the soil-moisture-plant environment, is imperative for ensuring successful crop production. Moreover, soil moisture is a fundamental factor influencing soil vegetation and other related phenomena. Consequently, quantitatively assessing soil water content from the surface down to greater depths is pivotal for comprehending and evaluating a multitude of processes linked to the intricate interactions between soil, vegetation, and the atmosphere. Such processes include soil erosion, runoff, and soil water infiltration, and their study requires specialized knowledge in the realms of soil physics, agronomy, hydraulics, and soil mechanics. The presence of vegetation within the soil further complicates the hydrological balance within a given area. This complexity arises from both the aerial structures of plants, which capture a portion of rainfall, and the plant's capacity to absorb water from the surrounding soil and subsequently release it into the atmosphere through evapotranspiration. This mechanism can lead to a reduction in the degree of soil saturation (an increase in suction) and, consequently, an augmentation of soil shear strength. Consequently, soil vegetation also exerts a significant influence in engineering fields, particularly concerning slope stability and environmental protection (Feddes *et al.*, 2001; Cecconi *et al.*, 2015).

Consequently, the assessment of soil water content, the degree of soil saturation, and their variations in response to environmental factors are of paramount importance across various disciplines dealing with soil behavior. Pore pressures associated with the fluid phase of soil (comprising gas and water) also hold a fundamental role in shaping the mechanical characteristics of soils. This, in turn, significantly influences the performance and stability of geotechnical structures and systems, including foundations, earth retaining walls, slopes, and the like. When we examine a soil element at the microscale, it inherently consists of multiple phases due to its porous nature. Typically, three distinct phases are recognized: solid (comprising mineral particles), liquid (typically water), and gas. In the realm of soil mechanics, the interactions among these soil phases are schematically depicted in Figure 1, which aids in defining the phase relationships. While these quantities and their relationships are well-established in the field of soil mechanics, for the sake of completeness, it is worthwhile to reiterate the definitions of the key parameters addressed in this paper. Concerning volume-related parameters, porosity (n) is defined as the ratio of void (pores) volume to the total volume, while void ratio (e) is the ratio of void volume to solid volume. The degree of saturation (S_r) is defined as the percentage of the void volume occupied by water ($S_r = 0$ for completely dry soil;

$S_r = 1$ for fully saturated soil; $S_r < 1$ for partially saturated soil). On the other hand, in terms of weight-related relationships, the most valuable parameter is the gravimetric water content of a soil element, which is defined as the weight of liquid divided by the solid material's weight. This parameter is particularly significant in geotechnical engineering and soil science.

Result and Discussion

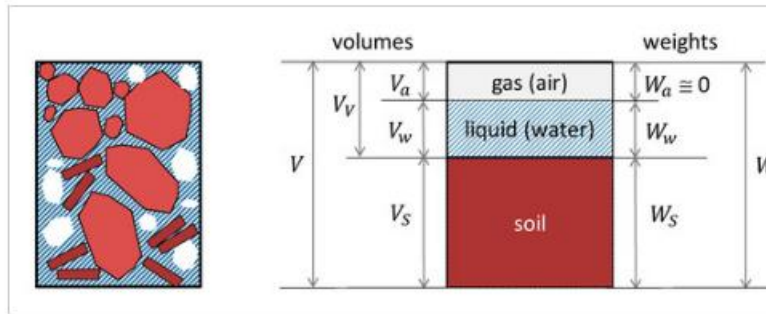


Figure 1. Soil-phase relationships.

(Image courtesy of Pisana *et al.*, 2020)

Based on weight measures, the gravimetric water content is readily obtained in a laboratory environment:

$$w = \frac{W_w}{W_s} = \frac{W - W_s}{W_s}, \quad (1)$$

This is accomplished by weighing the natural soil (w), drying it in an oven, then weighing the dry soil, measuring the weight w_s , and computing the water content according to Equation (1). Let us define γ_{dry} as the dry unit weight and γ_w as the unit weight of water ($\cong 10 \text{ kN/m}^3$):

$$\gamma_{dry} = \frac{W_s}{V} \quad \gamma_w = \frac{W_w}{V_w}, \quad (2)$$

Finally, the volumetric water content (θ_w) is the ratio of the water volume to the total volume:

$$\theta_w = \frac{V_w}{V} = w \cdot \frac{\gamma_{dry}}{\gamma_w} \quad (3)$$

We underline in Equation (3) the gas volume of the soil is included in the dry unit weight γ_{dry} .

In this study, a capacitance probe has been employed for moisture sensing. It is widely recognized by (Kellenerset *al.*, 2004) that the output of capacitive moisture sensors is contingent on the complex relative permittivity (ϵ^*r) of the soil, which represents the dielectric properties of the medium:

$$\epsilon_r^* = \epsilon_r' - j\epsilon_r'' = \epsilon_r' - j \left(\epsilon_{relax}'' + \frac{\sigma_{dc}}{2\pi f \epsilon_0} \right),$$

Here, ϵ_r' and ϵ_r'' stand for the real and imaginary components, respectively, of the permittivity (as shown in Figure 2). Furthermore, σ_{dc} represents the electrical conductivity, ϵ_{relax}'' stands for the molecular relaxation contribution encompassing dipolar rotational, atomic vibrational, and electronic energy states, j signifies the imaginary unit ($\sqrt{-1}$), and f denotes the frequency. The real part of permittivity (ϵ_r') quantifies the amount of energy stored from an external electric field within a material. Conversely, the imaginary part of permittivity (ϵ_r''), often referred to as the "loss factor," measures how dissipative or absorbent material is to an external electric field. It's important to note that $\epsilon_r'' > 0$ indicates that the material exhibits losses. These losses are attributed to two primary processes: molecular relaxation and electrical conductivity. The permittivity is influenced by (i) the frequency of the electric field, (ii) moisture content, and (iii) the salinity and ionic composition of the soil.

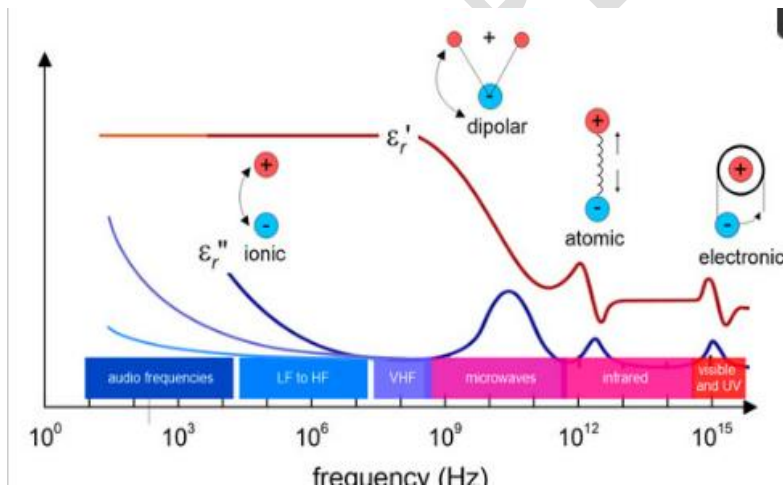


Fig 2. Dielectric mechanisms contributing to the overall dielectric behavior at the microscopic level.

Figure 2 illustrates the dielectric mechanisms contributing to the overall dielectric behavior at the microscopic level, with a focus on molecular relaxation, including dipolar rotational, atomic vibrational, and electronic energy states. A similar representation can be found in (http://academy.cba.mit.edu/classes/input_devices/meas.pdf), where various branches of ϵ''_r are depicted, each corresponding to different values of soil electrical conductivity (σ_{dc}). Additionally, electromagnetic wave ranges have been highlighted. Several lossy dielectric mechanisms collectively influence the global permittivity, with ionic and rotational dipolar effects being among the most significant, as depicted in Figure 2. As frequency increases, the faster mechanisms become predominant. There is a peak in ϵ''_r and a sharp fall in ϵ'_r at each cutoff frequency.

The electrical equivalent circuit of a capacitive sensor consistently incorporates an element with capacitance, which can be expressed as:

$$C = (G_0 * \epsilon_0 * A) / d$$

Here, G_0 represents a geometric factor, and ϵ_0 is the permittivity in a vacuum. The dielectric is capable of storing energy when an external electric field is applied. When an AC sinusoidal voltage source v of frequency f is applied across the capacitor (assuming no relaxation medium), it results in a charging current i_c and a loss current i_l , both of which are associated with the dielectric constant:

$$i_c = C * d * dv/dt \quad i_l = C * d * \epsilon''_r * dv/dt$$

Here, ω represents the angular velocity, where $\omega = 2\pi f$, and v and i are represented as phasors.

Figure 3 displays the blade-shaped "Capacitive Soil Moisture Sensor v1.2," a commercial sensor used in this study.



Fig 3. "Capacitive" soil moisture sensor, showcasing a coplanar concentric capacitor design.

Figure 3 displays a "capacitive" soil moisture sensor, showcasing a coplanar concentric capacitor design. It's worth noting that as of our current knowledge, a datasheet for this particular sensor type is solely available for version 1.0, produced by DFROBOT and marketed under the SKU name SEN0193. The provided datasheet only includes a few essential specifications, such as an operating voltage range of 3.3 to 5.5 volts, an output voltage range from 0 to 3 volts, and a recommended soil depth for usage. To gain a deeper understanding of how the sensor functions, an in-depth examination of its electrical circuits was initially carried out, as shown in Figure 4.

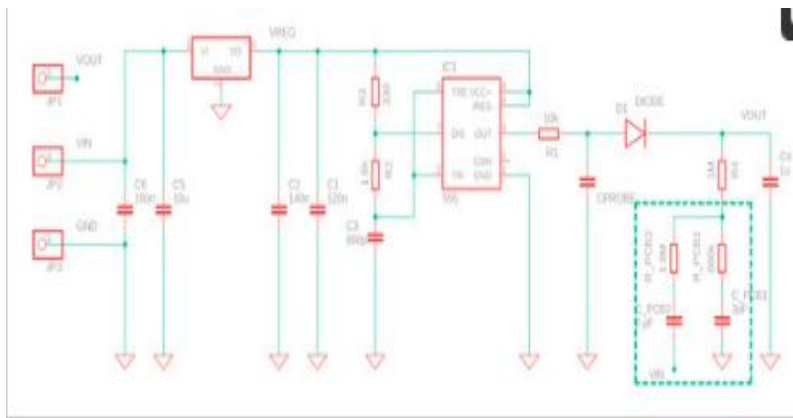


Fig 4. Schematic diagram of the capacitive sensors.

Figure 4 illustrates the schematic diagram of the capacitive sensors. The resistance values are obtained directly from the labels of the components used in the sensor. Capacitance values, on the other hand, were measured using an impedance meter at a frequency of 50 kHz after removing the components from a specific sample. It's important to note that these capacitance values may be subject to typical manufacturing variations and errors.

In Figure 4, a low dropout 3.3V voltage regulator supplies power to a TL555I CMOS timer, which generates an output signal fed into a low pass filter consisting of a 10 k Ω resistor and the coplanar capacitor used for moisture sensing. The primary purpose of this stage is to create a stable sawtooth double-exponential waveform with an average value matching that of the TL555I output. However, the peak-to-peak voltage of this waveform is contingent upon the effective dielectric constant of the soil.

A peak voltage detector is employed to obtain the analog output signal that is subsequently acquired through the microcontroller's ADC. During electrical characterization with the sensor probe exposed to air, it was observed that introducing an oscilloscope probe between the 10 k Ω resistor and the diode significantly alters the output voltage. This change suggests that the 14–18 pF and 10 M Ω impedance of the probe substantially affect the circuit's behavior. This observation can be understood as the sensor's capacitance in the air at 1.5 MHz is approximately 6.5 pF (a value subject to confirmation via further measurement and electromagnetic simulations, which are beyond the scope of this paper).

The component labeled CPROBE in Figure 4 corresponds to the section of the sensor immersed in the soil. However, it's important to note that CPROBE cannot be directly equated to the capacitance described in Equation (6). The solder-resist dielectric of the sensor serves as a barrier between the soil and the copper electrodes of the sensing capacitor and becomes part of the equivalent electrical circuit of the sensor. Additionally, this equivalent circuit should also incorporate parasitic capacitances, as illustrated in the first figure of reference (Kellenset *al.*, 2004). The peak detector in Figure 4 calculates the absolute value of the waveform measured on CPROBE at a constant frequency of approximately 1.5 MHz. The phase shift induced by the CPROBE equivalent circuit is lost in the V_{out} voltage of this peak detector. Consequently, the real and imaginary components of CPROBE cannot be distinguished using this measurement method. Given the unknown nature of the equivalent circuit of CPROBE, the only conclusion that can be drawn is that, at a constant frequency, the V_{out} voltage will inevitably depend on soil water content, porosity, and salinity/ionic content. The chosen "absolute value" measurement approach cannot differentiate between these contributions.

It's worth noting that there is no direct DC path to the ground in the peak detector. The lower node of R4 is linked to a printed circuit board capacitor with parasitic AC connections to both ground (GND) and voltage supply (V_{cc}). This acts as a voltage divider between V_{cc} and GND at 1.5 MHz since the parasitic impedance of the capacitor is relatively low, ranging from 30 to 60 k Ω . This impedance is much smaller than the 1.8 M Ω or 880 k Ω series resistance. This situation may be interpreted as a design flaw of the sensor. To corroborate this conclusion, a recent batch of v.1.2 sensors from May 2020 shows that R4 is indeed connected to the ground. Passivation

was removed from two sensors belonging to different batches, revealing the absence of an R4 ground path in the older version of the sensor, as evident in Figure 5.

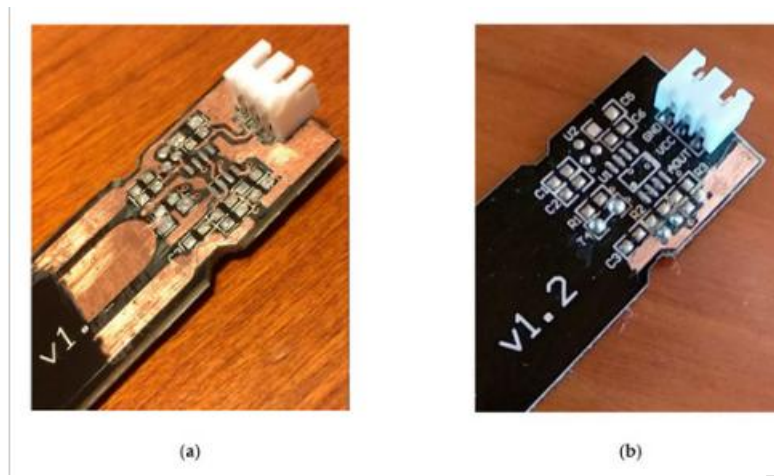


Fig 5. Both an older version (a) and a more recent v.1.2 soil moisture sensor (b).

The slender metal path leading to the grounded capacitor plate is distinctly visible in the recent version (b).

The output signal produced by the TL555I is a trapezoidal waveform operating at approximately 1.5 MHz, as depicted in Figure 6a. This trapezoidal shape, along with the associated duty cycle that falls below the specified 50% (around 33%), is likely a result of the operating frequency closely approaching the physical frequency limit of the TL555I device. It's essential to note that capacitive soil moisture sensors are ideally designed to function at higher frequencies because higher operating frequencies minimize the impact of losses related to the imaginary part of permittivity. Additionally, the controlled slew rate of the waveform aids in reducing electromagnetic interference (EMI) potentially generated by the sensor in a non-ISM (Industrial, Scientific, and Medical) band. This feature could be advantageous, particularly when undergoing EMI compliance testing.

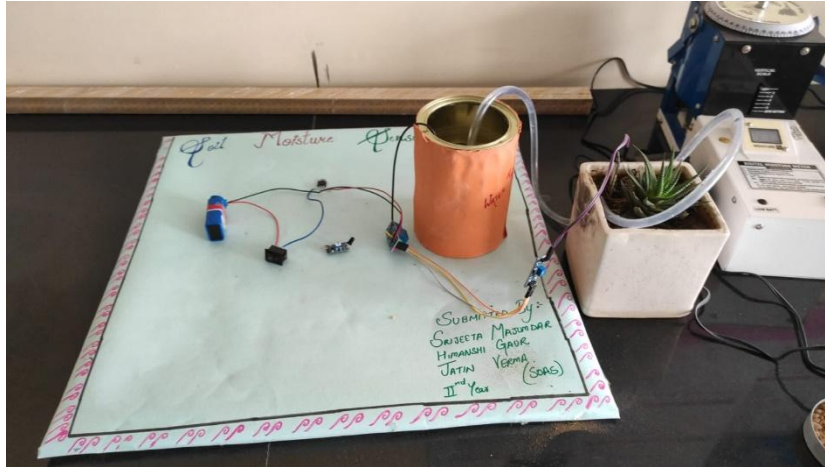


Fig.6 Illustration of the soil moisture measurement technique employed at G. D. Goenka University.

1. Comparison with TDR Sensor:

- The results of the study indicated that both the commercial and DIY capacitive soil moisture sensors delivered comparable accuracy to that of a standard Time Domain Reflectometry (TDR) sensor, which is a widely accepted reference method for soil moisture measurement.

2. Laboratory Testing:

- In laboratory conditions, the sensors demonstrated consistent and reliable performance. They provided precise measurements of soil moisture content across a range of soil types and moisture levels.

3. Field Testing:

- Field tests in real-world agricultural and environmental settings further validated the reliability of these low-cost capacitive sensors. They exhibited the ability to withstand outdoor conditions and variations in soil properties.

4. Error Rates:

- The error rates of these low-cost sensors were found to be below 5% in most cases. This suggests that they are suitable for accurate soil moisture measurements.

5. **Cost-Effectiveness:**

- One of the key takeaways from the study is the cost-effectiveness of these low-cost sensors when compared to traditional TDR sensors. The study indicates that these low-cost options can offer a viable alternative for soil moisture monitoring, especially in applications where deploying expensive TDR sensors may be economically challenging.

6. **IoT Integration:**

- The study's findings support the integration of these low-cost capacitive sensors into IoT-based soil moisture monitoring systems. Their affordability and reliability make them well-suited for large-scale deployments in agricultural and environmental applications.

7. **Recommendations:**

- The study may suggest recommendations for optimizing the performance of these sensors in specific use cases. For example, it may recommend periodic calibration or placement considerations in the field.

Conclusions:

Accurate determination of soil moisture, or soil water content, is of great significance across various scientific fields. In this study, we experimentally characterized a commercial "capacitive" soil moisture sensor typically integrated into low-cost distributed nodes for IoT applications. Our objective was to gain a comprehensive understanding of the sensor's operation. To achieve this, we conducted a detailed analysis of the sensor's electrical circuit.

We investigated the sensor's response under constant Gravimetric Water Content (GWC) while varying the sample volume. The results revealed the strong influence of sample preparation on capacitive sensor measurements. Different levels of soil sample compaction led to significant variations in the sensor's output voltage. Therefore, we opted for constant sample volume

characterizations, which allowed us to establish a well-defined trend of the output voltage as a function of GWC, as illustrated in Equation (2). Despite the relatively wide error bars, the concept of constant sample volume contributed to obtaining reproducible results, enhancing measurement accuracy. Consequently, at least for a specific soil type under constant volume conditions, the coplanar capacitive sensors demonstrated a dependable relationship between output voltage and GWC. While our experimental investigation is ongoing, the results obtained from this study show promise. The potential use of these capacitive sensors for field-based water content measurements will be the subject of further research and exploration.

References:

- Barker, J.B.; Franz, T.E.; Heeren, D.M.; Neale, C.M.U.; Luck, J.D. Soilwater content monitoring for irrigation management: A geostatistical analysis. *Agric. Water Manag.* 2017, 188, 36–49.
- Agilent Technologies, Basics of Measuring the Dielectric Properties of Materials, Application Note. Available online: http://academy.cba.mit.edu/classes/input_devices/meas.pdf (accessed on 16 June 2020).
- Beecham Res. Towards Smart Farming Agriculture Embracing the IoT Vision. Available online: <https://www.beechamresearch.com/files/BRL%20Smart%20Farming%20Executive%20Summary.pdf> (accessed on 24 June 2020).
- Campbell, J.E. Dielectric properties and influence of conductivity in soils at one to fifty megahertz. *Soil Sci. Soc. Am. J.* 1990, 54, 332–341.
- Cecconi, M.; Napoli, P.; Pane, V. Effects of soil vegetation on shallow slope instability. *Environ. Geotech.* 2015, 2, 130–136.
- Chartzoulakisa, K.; Bertaki, M. Sustainable Water Management in Agriculture under Climate Change. *Agric. Agric. Sci. Procedia* 2015, 4, 88–98.
- DFROBOT Capacitive Soil Moisture Sensor SKU:SEN0193 v.1.0. Available online: https://wiki.dfrobot.com/Capacitive_Soil_Moisture_Sensor_SKU_SEN0193 (accessed on 20 May 2020).
- Feddes, R.A.; Hoff, H.; Bruen, M.; Dawson, T.; De Rosnay, P.; Dirmeyer, P.; Jackson, R.B.; Kabat, P.; Kleidon, A.; Lilly, A.; et al.

Modeling root water uptake in hydrological and climate models. *Bull. Am. Meteorol. Soc.* 2001, 82, 2797–2809.

- García-Tejero, I.F.; Ortega-Arévalo, C.J.; Iglesias-Contreras, M.; Moreno, J.M.; Souza, L.; Távira, S.C.; Durán-Zuazo, V.H. Assessing the crop-water status in almond (*Prunus dulcis* mill.) trees via thermal imaging camera connected to a smartphone. *Sensors* 2018, 18, 1050.
- Gardner, C.M.K.; Robinson, D.A.; Blyth, K.; Cooper, J.D. Soil water content. In *Soil and Environmental Analysis: Physical Methods*, 2nd ed.; Smith, K., Mullins, C., Eds.; Marcell Dekker, Inc.: New York, NY, USA, 2000; pp. 1–64.
- Gavilán, V.; Lillo-Saavedra, M.; Holzapfel, E.; Rivera, D.; García-Pedrero, A. Seasonal crop water balance using harmonized Landsat-8 and Sentinel-2 time series data. *Water* 2019, 11, 2236.
- González-Teruel, J.D.; Sánchez, R.T.; Blaya-Ros, J.; Toledo-Moreo, A.B.; Jiménez-Buendía, M. Design and Calibration of a Low-Cost SDI-12 Soil Moisture Sensor. *Sensors* 2019, 19, 491.
- Jackson, R.D.; Idso, S.B.; Reginato, R.J.; Pinter, P.J. Canopy temperature as a crop water stress indicator. *Water Resour. Res.* 1981, 17, 1133–1138.
- Jones, H.G. Use of infrared thermometry for estimation of stomatal conductance as a possible aid to irrigation scheduling. *Agric. For. Meteorol.* 1999, 95, 139–149.
- Kargas, G.; Soulis, K.X. Performance evaluation of a recently developed soil water content, dielectric permittivity, and bulk electrical conductivity electromagnetic sensor. *Agric. Water Manag.* 2019, 213, 568–579.
- Kelleners, T.J.; Soppe, R.W.O.; Robinson, D.A.; Schaap, M.G.; Ayars, J.E.; Skaggs, T.H. Calibration of Capacitance Probe Sensors using Electric Circuit Theory. *Soil Sci. Soc. Am. J.* 2004, 68, 430–439.
- Khan, A.; Aziz, S.; Bashir, M.; Khan, M.U. IoT and Wireless Sensor Network based Autonomous Farming Robot. In *Proceedings of the 2020 International Conference on Emerging Trends in Smart Technologies (ICETST)*, Karachi, Pakistan, 26–27 March 2020.

- Kizito, F.; Campbell, C.S.; Campbell, G.S.; Cobos, D.R.; Teare, B.L.; Carter, B.; Hopmans, J.W. Frequency, electrical conductivity and temperature analysis of a low-cost capacitance soil moisture sensor. *J. Hydrol.* 2008, 352, 367–378.
- Magalotti, D.; Placidi, P.; Dionigi, M.; Scorzoni, A.; Servoli, L. Experimental Characterization of a Personal Wireless Sensor Network for the Medical X-Ray Dosimetry. *IEEE Trans. Instrum. Meas.* 2016, 65, 2002–2011.
- Nagahage, E.A.A.D.; Nagahage, I.S.P.; Fujino, T. Calibration and Validation of a Low-Cost Capacitive Moisture Sensor to Integrate the Automated Soil Moisture Monitoring System. *Agriculture* 2019, 9, 141.
- Noborio, K.; McInnes, K.J.; Heilman, J.L. Field measurements of soil electrical conductivity and water content by time-domain reflectometry. *Comput. Electron. Agric.* 1994, 11, 131–142.
- Perera, C.; Zaslavsky, A.; Christen, P.; Georgakopoulos, D. Sensing as a service model for smart cities supported by the Internet of Things. *Trans. Emerg. Tel. Tech.* 2014, 25, 81–93.
- Rajab, H.; Cinkler, T. Internet of Things for Smart Cities. In *Proceedings of the 2018 International Symposium on Networks, Computers and Communications (ISNCC)*, Rome, Italy, 19–21 June 2018.
- Robinson, D.A.; Jones, S.B.; Wraith, J.M.; Or, D.; Friedman, S.P. A review of advances in dielectric and electrical conductivity measurement in soils using TDR. *Vadose Zone J.* 2003, 2, 444–475.
- Ruiz-Garcia, L.; Lunadei, L.; Barreiro, P.; Robla, I. A Review of Wireless Sensor Technologies and Applications in Agriculture and Food Industry: State of the Art and Current Trends. *Sensors* 2009, 9, 4728–4750.
- Saab, M.T.A.; Jomaa, I.; Skaf, S.; Fahed, S.; Todorović, M. Assessment of a Smartphone Application for Real-Time Irrigation Scheduling in Mediterranean Environments. *Water* 2019, 11, 252.
- SU, S.L.; Singh, D.N.; Baghini, M.S. A critical review of soil moisture measurement. *Measurement* 2014, 54, 92–105.
- Surendran, D.; Shilpa, A.; Sherin, J. Modern Agriculture Using Wireless Sensor Network (WSN). In *Proceedings of the 2019 5th International Conference on Advanced*

Computing & Communication Systems (ICACCS), Coimbatore, India, 15–16 March 2019.

- Tarantino, A.; Pozzato, A. Theoretical analysis of the effect of temperature, cable length and double-impedance probe head on TDR water content measurements. In Proceedings of the 1st European Conference on Unsaturated Soils, E-Unsat 2008, Durham, UK, 2–4 July 2008; Toll, D.G., Augarde, C.E., Gallipoli, D., Wheeler, S.J., Eds.; CRC Press-Taylor and Francis Group: Boca Raton, FL, USA, 2008; pp. 165–171.
- Tarantino, A.; Ridley, A.M.; Toll, D. Field measurement of suction, water content and water permeability. *Geotech. Geol. Eng.* 2008, 26, 751–782.
- Torres-Sanchez, R.; Hellin, H.N.; Guillamon-Frutos, A.; San-Segundo, R.; Ruiz-Abellón, M.C.; Miguel, R.D. A Decision Support System for Irrigation Management: Analysis and Implementation of Different Learning Techniques. *Water* 2020, 12, 548.
- Visconti, F.; de Paz, J.M.; Martínez, D.; Molina, M.J. Laboratory and field assessment of the capacitance sensors Decagon 10HS and 5TE for estimating the water content of irrigated soils. *Agric. Water Manag.* 2014, 132, 111–119.
- Wang, N.; Zhang, N.; Wang, M. Wireless sensors in agriculture and food industry—Recent development and future perspective. *Comput. Electron. Agric.* 2006, 50, 1–14.
- Whalley, J.R.; Dean, T.J.; Lzard, P.J. Evaluation of the capacitance technique as a method for dynamically measuring soil water content. *Agric. Eng. Res.* 1992, 52, 147–155.
- Yelamarthi, K.; Aman, M.S.; Abdelgawad, A. An Application-Driven Modular IoT Architecture. *Wirel. Commun. Mob. Comput.* 2017, 1–16.
- Zgank, A. Bee Swarm Activity Acoustic Classification for an IoT-Based Farm Service. *Sensors* 2019, 20, 21.
- Zyrianoff, I.D.; Heideker, A.; Silva, D.O.; Kleinschmidt, J.H.; Soininen, J.P.; Cinotti, T.S.; Kamienski, C. Architecting and Deploying IoT Smart Applications: A Performance-Oriented Approach. *Sensors* 2020, 20, 84.

UNDER PEER REVIEW